



## Severe injury-induced osteoporosis and skeletal muscle mineralization: Are these related complications?

Stephanie N. Moore-Lotridge<sup>a,e,1</sup>, Rivka Ihejirika<sup>g,1</sup>, Breanne H.Y. Gibson<sup>a,f</sup>, Samuel L. Posey<sup>g</sup>, Nicholas A. Mignemi<sup>a</sup>, Heather A. Cole<sup>d</sup>, Gregory D. Hawley<sup>a</sup>, Sasidhar Uppuganti<sup>a,e,h</sup>, Jeffrey S. Nyman<sup>a,e,h</sup>, Jonathan G. Schoenecker<sup>a,b,c,e,f,\*</sup>

<sup>a</sup> Department of Orthopaedics, Vanderbilt University Medical Center, Nashville, TN 37232, USA

<sup>b</sup> Department of Pathology, Microbiology and Immunology, Vanderbilt University Medical Center, Nashville, TN 37232, USA

<sup>c</sup> Department of Pediatrics, Vanderbilt University Medical Center, Nashville, TN 37232, USA

<sup>d</sup> Department of Nuclear Medicine, Vanderbilt University Medical Center, Nashville, TN 37232, USA

<sup>e</sup> Center of Bone Biology, Vanderbilt University Medical Center, Nashville, TN 37232, USA

<sup>f</sup> Department of Pharmacology, Vanderbilt University, Nashville, TN 37232, USA

<sup>g</sup> Vanderbilt University Medical School, Vanderbilt University, Nashville, TN 37232, USA

<sup>h</sup> Tennessee Valley Healthcare System, Vanderbilt University, Nashville, TN 37232, USA

### ARTICLE INFO

#### Keywords:

Severe injury

Burn

Trauma

Soft tissue mineralization

Heterotopic ossification

Osteoporosis

Severe injury-induced osteoporosis

Biom mineralization

Dystrophic calcification

### ABSTRACT

Severely injured patients are beleaguered by complications during convalescence, such as dysregulated biomineralization. Paradoxically, severely injured patients experience the loss of bone (osteoporosis), resulting in diminished skeletal integrity and increased risk of fragility fractures; yet they also accrue mineralization in soft tissues, resulting in complications such as heterotopic ossification (HO). The pathophysiology leading to dysregulated biomineralization in severely injured patients is not well defined. It has been postulated that these pathologies are linked, such that mineralization is “transferred” from the bone to soft tissue compartments. The goal of this study was to determine if severe injury-induced osteoporosis and soft tissue calcification are temporally coincident following injury. Using a murine model of combined burn and skeletal muscle injury to model severe injury, it was determined that mice developed significant progressive bone loss, detectable as early as 3 days post injury, and marked soft tissue mineralization by 7 days after injury. The observed temporal concordance between the development of severe injury-induced osteoporosis and soft tissue mineralization indicates the plausibility that these complications share a common pathophysiology, though further experiments are required.

### 1. Background

Due to advances in critical care medicine, patients now survive severe injuries, such as burn, blast, or polytraumatic injuries, that were once considered fatal. While being fortunate to survive, many patient experience complications during convalescence, including poor tissue repair, and hemostasis (Gibson et al., 2020; Alessandrino and Balconi,

2013; Smith et al., 2000; Ferguson et al., 2008). While severely injured<sup>2</sup> patients are beleaguered by a variety of systemic derangements, one of the more paradoxical complications involves the dysregulation of biomineralization (Muschitz et al., 2017; Klein, 2006; Vanden Bossche and Vanderstraeten, 2005; Dey et al., 2017). Specifically, patients can experience a loss of mineralization from the skeleton, referred to as severe injury-induced osteoporosis, that diminishes skeletal integrity,

**Abbreviations:** HO, heterotopic ossification; DC, dystrophic calcification; CTX, cardiotoxin; STiCSS, soft tissue calcification scoring system; BMD, bone mineral density; DXA, dual energy X-ray absorptiometry;  $\mu$ CT, microcomputed tomography; BV/TV, bone volume/tissue volume; H&E, hematoxylin and eosin; DPI, days post injury.

\* Corresponding author at: 2200 Children’s Way, Nashville, TN 37232-9565, USA.

E-mail address: [jon.schoenecker@vumc.org](mailto:jon.schoenecker@vumc.org) (J.G. Schoenecker).

<sup>1</sup> Indicates that authors contributed equally

<sup>2</sup> “Severe injury” or “severely injured patients” refers to injuries that have a high risk for mortality. Examples include major mono- or poly-traumatic injuries, burns, blast, spinal cord injuries, traumatic brain injuries, etc.

<https://doi.org/10.1016/j.bonr.2020.100743>

Received 2 March 2020; Received in revised form 10 December 2020; Accepted 18 December 2020

Available online 26 December 2020

2352-1872/© 2020 The Authors.

Published by Elsevier Inc.

This is an open access article under the CC BY-NC-ND license

(<http://creativecommons.org/licenses/by-nc-nd/4.0/>).

delays rehabilitation, increases length of hospital stays, and increases the risk of fragility fractures (Kaewboonchoo et al., 2019; Fontaine and Herrmann, 1933). Furthermore, severely injured patients can also experience the accrual of mineralization in soft tissues such as skeletal muscle, resulting in complications such as dystrophic calcification (DC) and heterotopic ossification (HO). A recent report in *CTI* demonstrated that DC, if persistent within damaged skeletal muscle, is sufficient to promote HO formation (Moore-Lotridge et al., 2019), which clinically is associated with pain, joint dysfunction, and, in severe cases, may necessitate amputation of the affected limb (Dey et al., 2017; Kornhaber et al., 2017). Although estimates vary, it has been reported that up to 80% of patients develop HO after a severe injury. Furthermore, severe injury-induced HO has also complicated more than 60% of the severe orthopaedic extremity injuries during the Afghanistan and Iraq conflicts (Forsberg et al., 2009; Potter et al., 2006).

Following an injury, the acute phase response (APR) is activated in proportion to the injury severity (Gibson et al., 2020; Benvenuti et al., 2017; Baker et al., 2018). To ensure survival, the APR first activates coagulation and an acute inflammatory response to stop bleeding and prevent infection. Proportional to the amount of tissue injury, an exuberant survival inflammatory response following a severe injury can drive systemic changes in the musculoskeletal system (Gibson et al., 2020; Baker et al., 2018; Klein, 2019). Both pre-clinical and clinical studies have examined the molecular connections between traumatic injuries and hypermetabolism, skeletal muscle wasting, and rapid bone turnover (Klein, 2019; Pereira et al., 2005; Klein, 2015; Auger et al., 2017; Hew et al., 2020; Stanojcic et al., 2018). However, few studies have examined the relationship between severe injury-induced bone turnover, resulting in osteoporosis, and soft tissue calcification of injured tissues.

The overarching hypothesis of this study was that a shared pathophysiology exists, such that a “transfer” of mineralization from the bone to soft tissue compartments can occur. To determine if severe injury-induced osteoporosis and pathologic soft tissue calcification are mechanistically linked, we utilized a combined burn and skeletal muscle injury to model of severe injury. Unlike other preclinical severe injury models, burn injuries have a low risk of hemorrhage, thereby allowing for consistent investigation of the late complications of convalescence. This study aimed to examine if severe injury-induced osteoporosis and pathologic soft tissue calcification were temporally coincident. If found true, this temporal relationship may indicate a unifying pathophysiology between events and thereby provide the basis for future mechanistic and pharmacologic studies to help minimize soft tissue calcification in severely injured patients, such as combat veterans.

## 2. Materials and methods

### 2.1. Experimental overview

The overarching goal of this study was to examine, in a murine model of severe injury, if severe injury-induced osteoporosis and soft tissue calcification were temporally coincident, and therefore potentially pathologically connected. To examine this hypothesis, following a burn and/or skeletal muscle injury, bone quality and the presence of soft tissue calcification were assessed using both longitudinal and endpoint measures (Fig. 1).

### 2.2. Animal husbandry

All animal procedures were approved by Vanderbilt University IACUC and performed in accordance with ethical standards of the institution (M/15/024, M1800154). All studies were conducted in 6-week-old male C57BL/6J mice, weighing 20–25 g. Mice were individually housed in a regulated facility with 12-h light-dark cycle and provided food (SLOD chow) and water *ad libitum*.

### 2.3. Cardiotoxin-induced skeletal muscle injury mouse model

Skeletal muscle injury was induced by an intramuscular injection of 40  $\mu$ L of 10uM Cardiotoxin (CTX, Accurate Chemical and Scientific Corp; Westbury, NY) in the posterior compartments of the left and right lower limbs, as previously described (Moore-Lotridge et al., 2019; Mignemi et al., 2017; Moore et al., 2016).

### 2.4. Burn injury mouse model

This model was adapted from a separate burn wound model (Patil et al., 2017) and modified here to be conducted in conjunction with or without a skeletal muscle injury to the lower extremity to model severe injury. Following a subcutaneous injection of buprenorphine (0.5-mg/kg) 30 min prior to the burn procedure, mice were anesthetized with isoflurane and the dorsal hair was removed (Fig. 1A). Following hair removal, if the mouse was designated to receive a focal skeletal muscle injury, the gastrocnemius and soleus muscles were injected with CTX at this time (Fig. 1B). 1 ml of saline was injected subcutaneously posterior to the spine to protect the underlying spinal column from thermal injury (Fig. 1C). The mouse was then placed in a heat-resistant template (Fig. 1D & E) and partially submerged in a 100 °C water bath for 10 s to create a full thickness cutaneous burn covering approximately 30% of the total body surface area (Fig. 1F). Immediately following the burn, the mouse was dried and injected with 2 ml of intraperitoneal fluid resuscitation with lactated Ringer’s solution.

### 2.5. Radiographs

At 7, 14, 21, and 28 days post injury (DPI), mice were analyzed by digital radiography for the development of mineralization within the injured lower extremity as previously described (Fig. 1G) (Moore-Lotridge et al., 2019; Mignemi et al., 2017; Moore et al., 2016). Soft tissue mineralization was quantified using the previously validated soft tissue calcification scoring system (STiCSS) (Moore et al., 2016). Briefly, the operational definitions of each score are based on the percentage area of soft tissue calcification observed in the posterior compartment of the lower extremity: 0 (0%), 1 (1–25%), 2 (25–49%), 3 (50–75%) and 4 (>75%).

### 2.6. Longitudinal dual energy X-ray absorptiometry (DXA) imaging

Immediately prior to injury and at 1, 2, 5, 7, 14, 21, and 28 DPI, DXA imaging (Faxitron, LX-60) was obtained with an average of 3 images (Fig. 1G). Mice were laid in the prone position with their muzzle placed in a nose cone to maintain anesthetization. Legs of the mouse were placed laterally away from the body of the animal to obtain a clear image of the femurs. Scans were checked for quality, as movement of the mouse can result in aberrant measure. The whole femur was selected utilizing the arbitrary ROI analysis tool, and bone mineral density (BMD) values were obtained in  $\text{g}/\text{cm}^2$ . Measures from the left and right femurs from a single mouse were averaged together and reported as a single value within. As mice were not fasted as part of this study, vertebral measures were found to be unreliable due to the presence of food pockets (Shi et al., 2016).

### 2.7. Micro-computed tomography ( $\mu$ CT)

To more sensitively assess changes in bone quality,  $\mu$ CT imaging was performed on the distal femur, distinct from the site of skeletal muscle mineralization at 1, 3, 7, and 28 DPI (Fig. 1G), as previously described (Moore-Lotridge et al., 2019; Mignemi et al., 2017; Moore et al., 2016). The bone volume/tissue volume (BV/TV) ratio, trabecular thickness, trabecular space, and trabecular number were assessed within the metaphyseal region. Average cortical thickness, total cross sectional area, and tissue mineral density were assessed within the diaphyseal

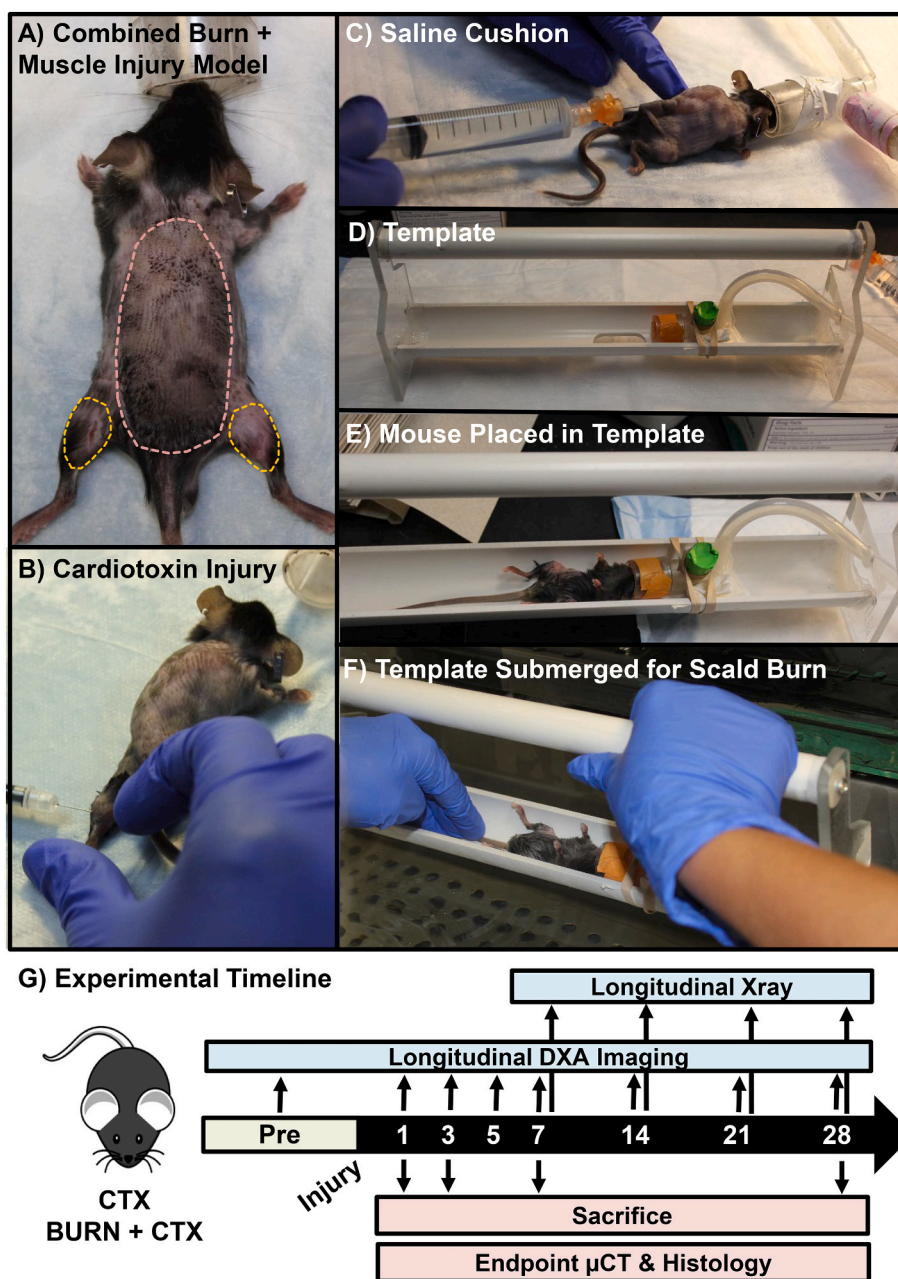


**Fig. 1.** Combined burn and skeletal muscle injury to model severe injury. To phenocopy the clinical condition of a severe injury, a A) 30% total body surface area full-thickness cutaneous burn was applied in combination with a remote focal skeletal muscle injury. Prior to burn injury, B) an intramuscular injection of cardiotoxin (CTX) is applied to the gastrocnemius and soleus muscles to induce a focal muscle injury. A medial approach is utilized to injure both the left and the right lower extremities prior to burn injury. C) Placement of a 1 ml subcutaneous saline cushion to protect the spine during burn injury. D) To control the burn region on the dorsum of the mouse, a heat resistant template is utilized. The mouse is placed in the template (E), and the template is partially submerged in a 100 °C water bath (F) for 10 s. G) Both longitudinal and end point assessments were carried out at 1, 3, 5, 7, 14, 21, or 28 days post injury as noted in the experimental timeline. Mice were sacrificed at 1, 3, 7, or 28 days post injury.

region (O'Neill et al., 2012). To visualize skeletal muscle mineralization,  $\mu$ CT imaging of the gastrocnemius and soleus muscles were conducted at 7 DPI as previously described (Moore-Lotridge et al., 2019; Mignemi et al., 2017; Moore et al., 2016).

## 2.8. Histologic analysis of skeletal muscle mineralization

Injured skeletal muscle was isolated at 7 and 28 DPI (Fig. 1G) and routinely fixed in 10% neutral-buffered formalin, processed, and embedded (Moore-Lotridge et al., 2019). 6  $\mu$ m sections were stained with hematoxylin and eosin (H&E) or von Kossa to visualize mineralization (Moore-Lotridge et al., 2019; Mignemi et al., 2017). At least 5 mice were analyzed per cohort/timepoint with >3 sections per mouse. Images included in manuscript represent the average result per cohort.

## 2.9. Statistical analysis

Differences in BMD from DXA assessment were assessed utilizing a 2-way ANOVA corrected for multiple comparisons. Differences in endpoint  $\mu$ CT parameters were assessed individually at each time point between cohorts and between 1 and 28 DPI in the same cohort by a non-parametric Mann-Whitney *U* test given that they are discrete samples. Difference in STICSS Score was analyzed with a non-parametric 1-way ANOVA corrected for multiple comparisons. Statistical analyses were performed in GraphPad Prism (v6, GraphPad Software, La Jolla, CA) with  $\alpha=0.05$ . Two-sided testing was applied throughout.  $N>3$  for all timepoints assessed. Significance reported was relative to adjusted *p* values where appropriate.



### 3. Results

#### 3.1. Severe injury-induced osteoporosis

In mice receiving a combined burn and CTX muscle injury (model of severe injury), significant bone loss was observed compared to mice receiving only a CTX muscle injury (lesser injury) (Fig. 2A). Longitudinal DXA imaging detected a significant reduction in average BMD of the left and right femurs by 7 DPI. Given that the mice examined are still undergoing bone development, a significant change in BMD between 5 and 28 DPI ( $p=0.050$ ) was observed in mice receiving a CTX injury, indicative of longitudinal bone growth. Alternatively, over the same time period, no change in BMD was observed in mice that received CTX + Burn injury ( $p=0.627$ ), leading to the greatest magnitude change in BMD between cohorts at 28 DPI (Fig. 2A). To more sensitively measure changes in bone quality and bone architecture, samples were collected and analyzed by  $\mu$ CT. By 3 DPI, a significant loss of percent metaphyseal bone volume/tissue volume, reduced trabecular thickness and trabecular number, and increase in trabecular space was detected in mice receiving CTX + Burn injury (Fig. 2B & C, Table 1). Assessment of cortical bone volume at 28 DPI between cohorts revealed a significant loss in the average cortical bone thickness in mice receiving CTX + Burn injury compared to unburned controls (CTX- $0.157 \pm 0.013$ ; Burn + CTX- $0.135 \pm 0.006$ ;  $p=0.001$ ), with no marked changes in total cross-sectional area of the diaphysis ( $p=0.279$ ) or tissue mineral density ( $p=0.493$ ).

#### 3.2. Skeletal muscle mineralization

By 7 DPI, marked skeletal muscle mineralization was observed in the gastrocnemius and soleus muscles by radiographic analysis and  $\mu$ CT reconstruction in mice that received CTX + Burn injury. Importantly, no significant mineralization was observed at any timepoint in mice that received either a focal skeletal muscle injury (CTX) or a burn injury alone (Fig. 3A). Histological analysis confirmed that the skeletal muscle mineralization observed at 7 and 28 DPI was morphologically indicative of DC (Fig. 3B) (Moore-Lotridge et al., 2019). Longitudinal radiographic analysis demonstrated that the deposited DC, while significantly greater in mice receiving CTX + Burn injury at 7 DPI, progressively regressed from injured muscle between 7 and 28 DPI resulting in comparable levels of mineralization to CTX controls by 28 DPI (Fig. 3C).

### 4. Discussion

This study identified that a temporal concordance exists in which both severe injury-induced osteoporosis and soft tissue mineralization occur. Specifically, progressive bone loss was observed as early as 3 DPI with  $\mu$ CT assessment and a subsequent gain in DC that was radiographically evident by 7 DPI. These results demonstrate the plausibility that a unifying pathophysiology may exist between these complications in which a “transfer” of mineralization from the bone to soft tissue compartments may occur, similar to what has been described previously in cardiac literature (Duke et al., 2016).

Under a homeostatic state, plasma contains near-saturating levels of calcium and phosphate (Moore et al., 2015). These levels are essential to allow for proper cellular signaling and to maintain musculoskeletal integrity. Yet, soft tissues are therefore, likewise exposed to these near-saturating levels and can experience pathologic mineralization if a nidus, such as tissue injury, occurs. Therefore, throughout life the body employs protective mechanisms, such as plasmin, pyrophosphate, and osteopontin, to block the mineralization within soft tissues (Kornhaber et al., 2017; Mignemi et al., 2017; Moore et al., 2015). As we age, in addition to accruing microtissue injuries, the body likewise experiences a diminished capacity to regulate biomineralization, leading to conditions such as calcific artery disease and osteoporosis (Sell and Scully, 1965; Giachelli, 1999; Mitsuyama et al., 2007; TEALE et al., 1989; Ettinger,

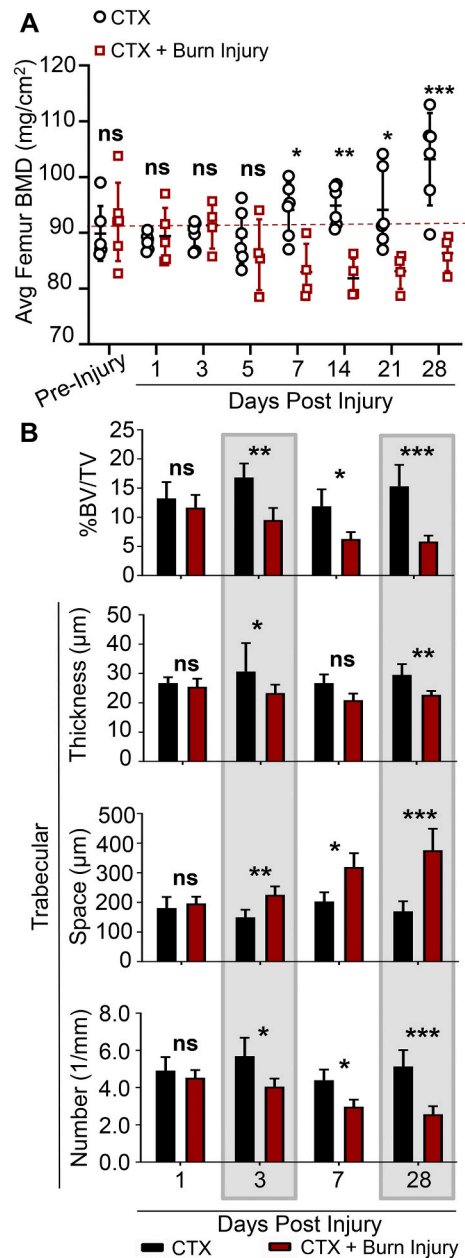


**Fig. 2.** Assessment of severe injury-induced osteoporosis in a murine model of combined burn and skeletal muscle injury. A) Pre-injury and post-injury DXA measures from 1 through 28 DPI. DXA measures of the left and right femurs were averaged and reported per mouse. B) To more sensitively assess bone architecture and bone loss, mice were sacrificed at 3, 5, 7, and 28 DPI, and the distal metaphysis was assessed for changes in trabecular bone, measured by % BV/TV, trabecular thickness, space between trabeculae, and trabecular number. Please see Table 1 for detailed statistical analysis and N. C) 2D cross section of the distal metaphysis of the femur in the XY plane. Yellow arrows indicate areas of reduced trabecular bone. Error bars represent mean  $\pm$  SD in all images. \* notes significance ( $p$ ) less than 0.05, \*\* $p < 0.01$ , \*\*\* $p < 0.001$ .

**Table 1**

Detailed statistical analysis of trabecular and cortical bone loss between mice receiving a combined burn and skeletal muscle injury (Burn + CTX; model of severe injury) or muscle injury alone (CTX; lesser injury) measured by endpoint  $\mu$ CT analysis. \* notes significance (P) less than 0.05, \*\*p<0.01, \*\*\*p<0.001.

	1 DPI		3 DPI		7 DPI		28 DPI		Analysis between 1 and 28 DPI	
	CTX (N=5)	CTX $\pm$ Burn (N=7)	CTX (N=5)	CTX $\pm$ Burn (N=6)	CTX (N=3)	CTX $\pm$ Burn (N=6)	CTX (N=10)	CTX $\pm$ Burn (N=10)	CTX	CTX $\pm$ Burn
%BV/TV	13.3 $\pm$ 2.8	16.6 $\pm$ 2.2	16.8 $\pm$ 0.024	9.5 $\pm$ 2.1**	11.9 $\pm$ 2.9	6.3 $\pm$ 1.2*	15.3 $\pm$ 3.7	5.8 $\pm$ 1.0***	ns, p=0.636	***, p<0.001
Trabecular thickness ( $\mu$ m)	27 $\pm$ 2	26 $\pm$ 3	31 $\pm$ 10	23 $\pm$ 3*	27 $\pm$ 3	21 $\pm$ 2	30 $\pm$ 4	23 $\pm$ 1**	ns, p=0.723	ns, p=0.622
Trabecular space ( $\mu$ m)	181 $\pm$ 37	197 $\pm$ 22	150 $\pm$ 26	225 $\pm$ 29**	203 $\pm$ 31	319 $\pm$ 47*	170 $\pm$ 34	376 $\pm$ 72***	ns, p=0.998	***, p<0.001
Trabecular number (1/mm)	4.92 $\pm$ 0.72	4.54 $\pm$ 0.41	5.69 $\pm$ 0.99	4.06 $\pm$ 0.43*	4.40 $\pm$ 0.57	2.98 $\pm$ 0.38*	5.14 $\pm$ 0.88	2.57 $\pm$ 0.43***	ns, p=0.988	***, p<0.002

2003). Given these temporal changes under homeostatic conditions, it is also possible that age may influence the body's capacity to regulate biomineralization following a severe injury. This is observed in both burn patients and those with traumatic injuries, where the incidence of HO is estimated to be lower in pediatric patients compared to adults with injuries of similar severity (Kluger et al., 2000; Hurvitz et al., 1992; Orchard et al., 2015; Gaur et al., 2003; Bossche and Vanderstraeten, 2005). Interestingly, reports from veterans suffering polytraumatic injuries indicates that a lower age, specifically <30 years of age, was independently predictive of heterotopic ossification development on multivariate analysis (Forsberg et al., 2009). While many mechanisms can influence this change in incidence, further studies characterizing the capacity for protection mechanisms to regulate biomineralization throughout life may provide critical insight and pharmacologic direction.

Severe injuries such as burn or polytraumas can lead to the systemic derangement of multiple body systems including coagulation, inflammation, and the immune system (Muschitz et al., 2017; Klein, 2019; Hew et al., 2020; Smolle et al., 2017; Peterson et al., 2015). Given the quick onset of bone loss following severe injuries, prior studies have attributed bone loss to a variety of mechanisms including endogenous glucocorticoids, production of pro-inflammatory cytokines, progressive vitamin D deficiency, and disruption of calcium homeostasis (Klein, 2019; Muschitz et al., 2016). Independent of the mechanism, numerous studies have illustrated that release of calcium, phosphate, and magnesium from the bone can have systemic effects on muscle physiology, regulation of inflammation, and glucose handling. To date, few investigations have examined how severe injuries can predispose soft tissues to pathologic mineralization. Given the temporal concordance between the development of osteoporosis and soft tissue calcification, it is plausible that a severe injury can 1) drive bone-turnover, thereby increasing the availability of calcium and phosphate in the plasma (Klein, 2019; Liseicki et al., 2018) and 2) simultaneously diminish soft tissue protection mechanisms against calcification (Gibson et al., 2017; Caprini et al., 1977; García-Avello et al., 1998; Ball et al., 2020); thereby establishing an environment in damaged skeletal muscle where DC formation is favorable. Given the plausibility of these complications sharing a common pathophysiology, further experiments investigating a "transfer of compartment" hypothesis is warranted. If found to be true, pharmacologic interventions aimed at reducing bone turn over may likewise reduce the risk of soft tissue calcification; thereby adding to the growing body of literature illustrating the potential clinical benefit of administering anti-catabolic agents in patients following severe injuries later in convalescence (Børsheim et al., 2014; Pin et al., 2019).

While previously thought to be distinct pathologies, a prior study demonstrated that DC formation within skeletal muscle, if persistent, is sufficient to form HO (Moore-Lotridge et al., 2019). Here, progressive regression of DC from skeletal muscle was observed over 28DPI, indicating that the regressive mechanisms, previously determined to act through macrophage phagocytosis (Moore-Lotridge et al., 2019), are

still functioning in our model. However, if the severity of the injury was increased or comorbidities were added to the model, both of which are linked to reduced macrophage function, DC regression may be impaired, leading to the possible formation of HO.

Injury is an essential component of skeletal muscle mineralization and the formation of HO. While clinical studies have detected the development of mineralization in muscle following a burn injury (Kornhaber et al., 2017), the location of these mineralized deposits is often unpredictable, making them difficult to reliably detect and track longitudinally. Unlike patients clinically, the ability to control essential variables is possible in a pre-clinical animal model. For example, the location of injury can be controlled in a pre-clinical animal model, allowing researchers to better predict the location of skeletal muscle mineralization. Yet, when utilizing an animal model of disease, one should consider the ability of the model to phenocopy the clinical condition and outcomes to support translation of associated findings.

## 5. Conclusion

By utilizing a murine model of combined burn and skeletal muscle injury as a model of severe injury, this study effectively examined late complications of convalescence, specifically dysregulated biomineralization. This study found that a temporal concordance exists in which both severe injury-induced osteoporosis and soft tissue mineralization occur. Going forward, future studies are required to investigate potential mechanistic links between severe injury-induced osteoporosis and soft tissue mineralization, as well as potential therapeutic interventions for mitigating dysregulated biomineralization. The murine model presented within this manuscript can be utilized in such mechanistic studies, providing the foundation for future clinically translatable work.

## CRedit authorship contribution statement

SNML contributed to study design, data collection, manuscript preparation, statistical analysis, and figure development.

RI assisted in study design, model development, and data collection.

BHYG and SLP contributed to data collection, manuscript revisions, and figure development. NAM assisted in study design and model development.

HAC assisted with critical manuscript revisions, data analysis, and figure development.

GDH and SU assisted with data collection and manuscript revisions.

JSN provided critical expertise for study design, data analysis, and manuscript revisions.

JGS oversaw the completion of this project, obtained funding, directed study design and data analysis.

All authors reviewed the paper critically for intellectual content and approved the final version. All authors agree to be accountable for the work and to ensure that any questions relating to the accuracy and integrity of the paper are investigated and properly resolved.

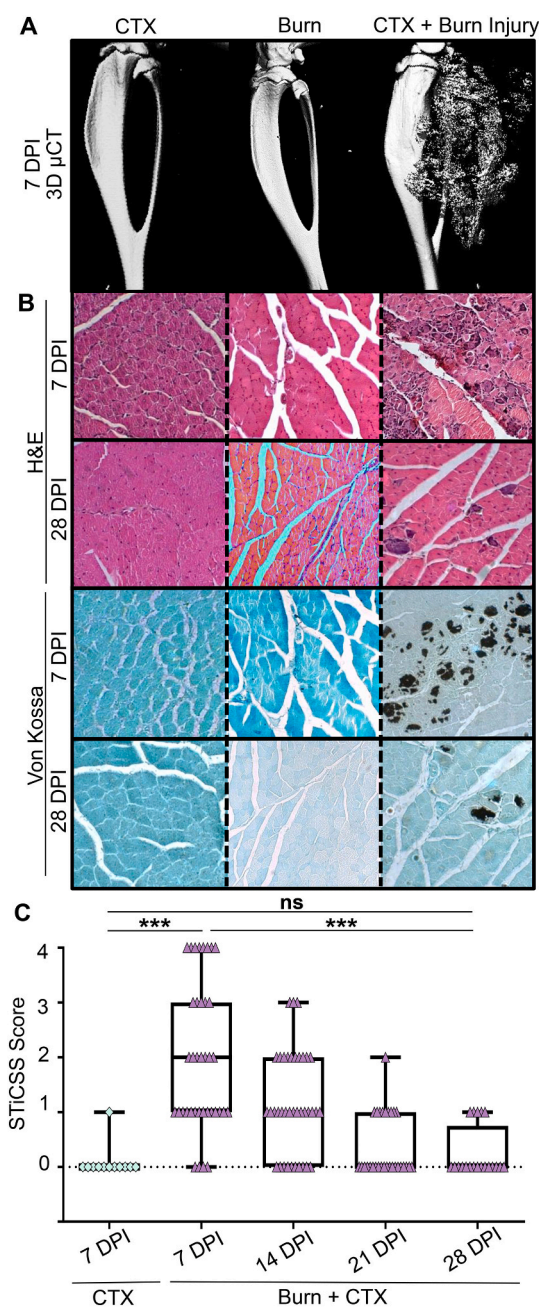


**Fig. 3.** Assessment of skeletal muscle mineralization in a murine model of combined burn and skeletal muscle injury. A) By 7 DPI, marked skeletal muscle mineralization was radiographically evident by 3D  $\mu$ CT reconstruction. B) Representative histologic analysis is morphologically indicative of dystrophic calcification.  $N \geq 3$  for each cohort. C) Longitudinal radiographic assessment and STiCSS scoring in mice undergoing CTX or CTX + Burn injury. Given that both the left and right lower limb is injury, each point upon the graph represents a single limb. STiCSS: CTX: 7DPI -  $N=12$  limbs assessed. CTX + Burn injury: 7DPI -  $N=38$  limbs assessed, 14 DPI -  $N=38$  limbs, 21 DPI -  $N=30$  limbs, 28 DPI -  $N=20$  limbs. Error bars represent median + interquartile range. \* notes significance ( $p$ ) less than 0.05, \*\*\*  $p < 0.001$ .

#### Transparency document

The [Transparency document](#) associated with this article can be found, in online version.

#### Declaration of competing interest

The authors declare the following financial interests/personal relationships which may be considered as potential competing interests:

Dr. Moore-Lotridge has no known competing financial interests or personal relationships that could have appeared to influence the work reported in this paper.

Dr. Ihejirka has no known competing financial interests or personal relationships that could have appeared to influence the work reported in this paper.

Ms. Gibson has no known competing financial interests or personal relationships that could have appeared to influence the work reported in this paper.

Dr. Posey is a member of the U.S. Air Force. The views expressed in this article are those of the author and do not reflect the official policy or position of the United States Air Force, Department of Defense, or the U.S. Government.

Dr. Mignemi has no known competing financial interests or personal relationships that could have appeared to influence the work reported in this paper.

Dr. Cole has no known competing financial interests or personal relationships that could have appeared to influence the work reported in this paper.

Mr. Hawley has no known competing financial interests or personal relationships that could have appeared to influence the work reported in this paper.

Mr. Uppuganti has no known competing financial interests or personal relationships that could have appeared to influence the work reported in this paper.

Dr. Nyman has no known competing financial interests or personal relationships that could have appeared to influence the work reported in this paper.

Dr. Schoencker is a member of the education advisory board at OrthoPediatrics, receives research funding from OrthoPediatrics, and research support from IONIS Pharmaceuticals, PXE International, the United States Department of Defense, and the National Institutes of Health.

#### Acknowledgements

This research was conducted in conjunctions with the Vanderbilt University School of Medicine Research Immersion Program. The authors would like to thank the members of the Schoencker Lab, in particular Jacob Schultz and Zack Backstrom, the Vanderbilt University Bone Center, and Dr. Corey Lotridge for their assistance reviewing this work. Finally, we would like to thank our family, friends, and academic colleagues for their continual encouragement and support.

#### Funding

For this work was provided by the National Institutes of Health ([1R01GM126062-01A1, NIGMS, JGS], [T32GM007628, NIGMS, SNML], [T32AR059039, NIAMS, BGHY], [1F31HL149340, NHLBI, BGHY], [3R03AR065762-01A1S1, NIAMS, RI]), the Vanderbilt University Medical Center Department of Orthopaedics and Rehabilitation (JGS), the Jeffrey W. Mast Chair in Orthopaedics Trauma and Hip Surgery (JGS), and the Caitlin Lovejoy Fund (JGS). Use of the Translational Pathology Shared Resource was supported by NCI/NIH Cancer Center Support Grant (2P30 CA068485-14) and the Vanderbilt Mouse Metabolic Phenotyping Center Grant (5U24DK059637-13).  $\mu$ CT imaging and analysis were supported in part by the Center for Small Animal Imaging at the Vanderbilt University Institute of Imaging Sciences (S10RR027631) from the NIH. Funding sources for this project had no involvement in study design, collection and analysis of data, writing of



the report, or decision in submitting this article for publication.

## References

- Alessandrino, F., Balconi, G., 2013. Complications of muscle injuries. *J. Ultrasound* 16 (4), 215–222.
- Auger, C., Samadi, O., et al., 2017. The biochemical alterations underlying post-burn hypermetabolism. *Biochimica et Biophysica Acta (BBA)-Molecular Basis of Disease* 1863 (10), 2633–2644.
- Baker, C.E., Moore-Lotridge, S.N., et al., 2018. Bone fracture acute phase response—a unifying theory of fracture repair: clinical and scientific implications. *Clin. Rev. Bone Mineral Metab.* 16 (4), 142–158.
- Ball, R.L., Keyloun, J.W., et al., 2020. Burn-induced coagulopathies: a comprehensive review. *Shock* 54 (2), 154–167.
- Benvenuti, M., An, T., et al., 2017. Double-edged sword: musculoskeletal infection provoked acute phase response in children. *Orthop. Clin.* 48 (2), 181–197.
- Børshiem, E., Herndon, D.N., et al., 2014. Pamidronate attenuates muscle loss after pediatric burn injury. *J. Bone Miner. Res.* 29 (6), 1369–1372.
- Bossche, L.V., Vanderstraeten, G., 2005. Heterotopic ossification: a review. *J. Rehabil. Med.* 37 (3), 129–136.
- Caprini, J.A., Lipp, V., et al., 1977. Hematologic changes following burns. *J. Surg. Res.* 22 (6), 626–635.
- Dey, D., Wheatley, B.M., et al., 2017. The traumatic bone: trauma-induced heterotopic ossification. *Transl. Res.* 186, 95–111.
- Duke, J.M., Randall, S.M., et al., 2016. Understanding the long-term impacts of burn on the cardiovascular system. *Burns* 42 (2), 366–374.
- Ettinger, M.P., 2003. Aging bone and osteoporosis: strategies for preventing fractures in the elderly. *Arch. Intern. Med.* 163 (18), 2237–2246.
- Ferguson, M., Brand, C., et al., 2008. Outcomes of isolated tibial shaft fractures treated at level 1 trauma centres. *Injury* 39 (2), 187–195.
- Fontaine, R., Herrmann, L.G., 1933. Post-traumatic painful osteoporosis. *Ann. Surg.* 97 (1), 26.
- Forsberg, J.A., Pepek, J.M., et al., 2009. Heterotopic ossification in high-energy wartime extremity injuries: prevalence and risk factors. *JBJS* 91 (5), 1084–1091.
- García-Avello, A., Lorente, J.A., et al., 1998. Degree of hypercoagulability and hyperfibrinolysis is related to organ failure and prognosis after burn trauma. *Thromb. Res.* 89 (2), 59–64.
- Gaur, A., Sinclair, M., et al., 2003. Heterotopic ossification around the elbow following burns in children: results after excision. *JBJS* 85 (8), 1538–1543.
- Giachelli, C.M., 1999. Ectopic calcification: gathering hard facts about soft tissue mineralization. *Am. J. Pathol.* 154 (3), 671–675.
- Gibson, B., Moore-Lotridge, S., et al., 2017. The consumption of plasminogen following severe burn and its implications in muscle calcification. *The FASEB Journal* 31 (1 supplement), 390–394.
- Gibson, B.H., Duvernay, M.T., et al., 2020. Plasminogen activation in the musculoskeletal acute phase response: injury, repair, and disease. *Res. Pract. Thromb. Haemost.* 4 (4), 469–480.
- Hew, J.J., Parungao, R.J., et al., 2020. Mouse models in burns research: characterisation of the hypermetabolic response to burn injury. *Burns* 46 (3), 663–674.
- Hurvitz, E.A., Mandac, B.R., et al., 1992. Risk factors for heterotopic ossification in children and adolescents with severe traumatic brain injury. *Arch. Phys. Med. Rehabil.* 73 (5), 459–462.
- Kaewboonchoo, O., Sung, F.C., et al., 2019. Risk of osteoporosis and fracture in victims with burn injury. *Osteoporos. Int.* 30 (4), 837–843.
- Klein, G.L., 2006. Burn-induced bone loss: importance, mechanisms, and management. *J. Burns Wounds* 5, e5.
- Klein, G.L., 2015. Disruption of bone and skeletal muscle in severe burns. *Bone Res.* 3, 15002.
- Klein, G.L., 2019. The role of the musculoskeletal system in post-burn hypermetabolism. *Metabolism* 97, 81–86.
- Kluger, G., Kochs, A., et al., 2000. Heterotopic ossification in childhood and adolescence. *J. Child Neurol.* 15 (6), 406–413.
- Kornhaber, R., Foster, N., et al., 2017. The development and impact of heterotopic ossification in burns: a review of four decades of research. *Scars Burn Healing* 3, 2059513117695659.
- Lisiecki, J., Levi, B., et al., 2018. Importance of mineral and bone metabolism after burn. In: *Total Burn Care*. Elsevier, pp. 268–275.e2.
- Mignemi, N.A., Yuasa, M., et al., 2017. Plasmin prevents dystrophic calcification after muscle injury. *J. Bone Miner. Res.* 32 (2), 294–308.
- Mitsuyama, H., Healey, R.M., et al., 2007. Calcification of human articular knee cartilage is primarily an effect of aging rather than osteoarthritis. *Osteoarthr. Cartil.* 15 (5), 559–565.
- Moore, S.N., Tanner, S.B., et al., 2015. Bisphosphonates: from softening water to treating PXE. *Cell Cycle* 14 (9), 1354–1355.
- Moore, S.N., Hawley, G.D., et al., 2016. Validation of a radiography-based quantification designed to longitudinally monitor soft tissue calcification in skeletal muscle. *PLoS One* 11 (7), e0159624.
- Moore-Lotridge, S.N., Li, Q., et al., 2019. Trauma-induced nanohydroxyapatite deposition in skeletal muscle is sufficient to drive heterotopic ossification. *Calcif. Tissue Int.* 104 (4), 411–425.
- Muschitz, G.K., Schwabegger, E., et al., 2016. Early and sustained changes in bone metabolism after severe burn injury. *J. Clin. Endocrinol. Metab.* 101 (4), 1506–1515.
- Muschitz, G.K., Schwabegger, E., et al., 2017. Long-term effects of severe burn injury on bone turnover and microarchitecture. *J. Bone Miner. Res.* 32 (12), 2381–2393.
- O'Neill, K.R., Stutz, C.M., et al., 2012. Micro-computed tomography assessment of the progression of fracture healing in mice. *Bone* 50 (6), 1357–1367.
- Orchard, G.R., Paratz, J.D., et al., 2015. Risk factors in hospitalized patients with burn injuries for developing heterotopic ossification—a retrospective analysis. *J. Burn Care Res.* 36 (4), 465–470.
- Patil, N.K., Bohannon, J.K., et al., 2017. Flt3 ligand treatment attenuates T cell dysfunction and improves survival in a murine model of burn wound sepsis. *Shock* 47 (1), 40–51.
- Pereira, C., Murphy, K., et al., 2005. Post burn muscle wasting and the effects of treatments. *Int. J. Biochem. Cell Biol.* 37 (10), 1948–1961.
- Peterson, J.R., Eboda, O.N., et al., 2015. Effects of aging on osteogenic response and heterotopic ossification following burn injury in mice. *Stem Cells Dev.* 24 (2), 205–213.
- Pin, F., Bonetto, A., et al., 2019. Molecular mechanisms responsible for the rescue effects of pamidronate on muscle atrophy in pediatric burn patients. *Front. Endocrinol.* 10, 543.
- Potter, B.K., Burns, T.C., et al., 2006. Heterotopic ossification in the residual limbs of traumatic and combat-related amputees. *JAAOS J. Am. Acad. Orthop. Surg.* 14 (10), S191–S197.
- Sell, S., Scully, R.E., 1965. Aging changes in the aortic and mitral valves. histologic and histochemical studies, with observations on the pathogenesis of calcific aortic stenosis and calcification of the mitral annulus. *Am. J. Pathol.* 46 (3), 345–365.
- Shi, J., Lee, S., et al., 2016. Guidelines for dual energy X-ray absorptiometry analysis of trabecular bone-rich regions in mice: improved precision, accuracy, and sensitivity for assessing longitudinal bone changes. *Tissue Eng. C Methods* 22 (5), 451–463.
- Smith, G.S., Dannenberg, A.L., et al., 2000. Hospitalization due to injuries in the military: evaluation of current data and recommendations on their use for injury prevention. *Am. J. Prev. Med.* 18 (3), 41–53.
- Smolle, C., Cambiaso-Daniel, J., et al., 2017. Recent trends in burn epidemiology worldwide: a systematic review. *Burns* 43 (2), 249–257.
- Stanojic, M., Abdullahi, A., et al., 2018. Pathophysiological response to burn injury in adults. *Ann. Surg.* 267 (3), 576–584.
- TEALE, C., ROMANIUK, C., et al., 1989. Calcification on chest radiographs: the association with age. *Age Ageing* 18 (5), 333–336.
- Vanden Bossche, L., Vanderstraeten, G., 2005. Heterotopic ossification: a review. *J. Rehabil. Med.* 37 (3), 129–136.